

DENSITY FUNCTIONAL THEORY TO STUDY STOPPING POWER OF PROTON IN WATER, LUNG, BLADDER, AND INTESTINE

Wejdan A. Jasim¹ and Rashid O. Kadhim²

^{1,2} Department of Physics, College of Education for Girls, University of Kufa, Najaf, Iraq.
Email: ¹ sitwijdan2014@gmail.com, ² rashid.alghnimi@uokufa.Edu.iq

DOI: 10.17605/OSF.IO/549RZ

Abstract

The study examined water and human tissue mean ionization potential and stopping power. Gaussian 09W calculated base set mean ionization potentials. The charge density distribution of orbital electrons in water and tissue atoms was examined to determine the proton energy. The Bethe formula and density functional theory determined water, lung, bladder, and gut stopping power, range, and time. Figure 1 shows the SRIM-2013 program's stopping power calculations and their theoretical counterparts. Proton energy raised stopping power to a maximum, then dropped. SRIM-2013 and the current study showed high correlation. Table 2 shows water and tissue element weight ratios, while Table 3 shows stopping power calculations (S_{total}) for different proton energies. Figures 2 and 3 demonstrate the correlation coefficients between SRIM-2013 and theoretical range and stopping time calculations. The research showed that stopping power rises at low energies (<0.1 MeV) and diminishes at higher energies (>0.1 MeV). When applying the Bethe equation to determine the total stopping power in the examined tissues, the results matched the practical findings of the SRIM-2013 software with equivalent correlation coefficients ($R_c = 0.9$).

Keywords: Density Functional Theory (DFT), Stopping Power, Range, Stopping Time, Mean Ionization Potential, SRIM-2013 Program, Human Body Tissues.

1. INTRODUCTION

Radiotherapy utilizes proton beams to effectively treat malignant tumors. To accurately determine the radiation dosage of proton therapy, it is crucial to have a comprehensive understanding of the stopping power and range values of protons in different materials [1-7]. Calculating the stopping power and range of charged particles in matter has long been a subject of experimental and theoretical interest. Precise knowledge of stopping power and range values for protons is essential in various fields, including radiation physics, chemistry, medicine, microdosimetry, proton therapy, and biology. Understanding the stopping power and range data is particularly important for evaluating phantom materials and radiation detector materials [8]. Previous studies have investigated the range and stopping power of protons in various organic materials [9, 10]. However, there is a limited amount of research that specifically includes bodily tissues, which is crucial for proton therapy. In the case of protons, the electronic stopping power, resulting from inelastic collisions with the target's electrons, contributes significantly to the overall stopping power, while nuclear stopping power becomes relevant only at extremely high energies.

2. THEORY

The effective charge Z_2^* of projectiles was introduced by Bohr [12] and is the best extending formula for average energies. W. Brandt and Yarlagadda et al. [13, 14] The Bohr abstraction criterion has been extensively explained in detail. According to this criterion, the moving ion removes all outer shell electrons from the target atom, which are bound in orbitals with velocities less than a certain value, denoted as u . It is important to note that this criterion applies to both the moving ion and the target atom,

considering the symmetry between them. In order to accurately apply the criterion, the effective atomic number of the target electrons, denoted as Z_2^* , and the effective mean excitation energy, denoted as I^* , need to be taken into account. These parameters depend on the energy of the moving ion.

At higher energies, the cumulative corrections for Z_2^* and I^* should be considered, which are generally similar to the inner shell corrections. However, it should be noted that the values of I^* deviate from the values of I , which are typically assumed to be independent of energy. To incorporate these considerations, the modified Bethe formula is rewritten accordingly [15].

$$S_e = \frac{4\pi(Z_1^*)^2 e^4 N}{mv^2} Z_2^* \ln\left(\frac{2mv^2}{I^*}\right) \quad (1)$$

therefore the effective number of atoms Z^* (Z_1 and Z_2) can be determined from [16];

$$Z^* = 4\pi \int_{r_b}^{\infty} r^2 \rho(r) dr \quad (2)$$

where r is distance from the nucleus, r_b is determined from Bohr stripping criterion $v \geq bv_F(r_b) = b\hbar[3\pi^2\rho(r_b)]^{1/3}$ where $v_F(r)$ stand for the velocity of the projectile or target atom's Thomas-Fermi orbital, b is a proportional constant of around 1.26, and $\rho(r)$ represents the electronic charge density distribution in the atom. According to the Lindhard and Scharff hypothesis, the effective mean excitation energy I is [17].

$$\ln I^* = \frac{4\pi}{Z_2^*} \int_{r_b}^{\infty} \ln[\gamma\hbar\omega_p(r)] r^2 \rho(r) dr \quad (3)$$

where $\gamma = \sqrt{2}$ for $Z \geq 30$ and $\omega_p(r)$ is the local plasma frequency $(4\pi e^2 \rho(r)/m)^{1/2}$. Lindhard and Scharff proposed a criterion; $2mv^2 \geq \gamma\hbar\omega_p(r)$, but Bohr criterion is preferable for the present purpose.

Stopping power of composites and tissues is given as sum of S.T.P. of its constituent elements according to Bragg equation [18].

$$S_{com.}(E) = \sum_i w_i S_i(E) \quad (4)$$

Where w_i is weight ratio of each element in compound, and $S_i(E)$ is stopping power in element.

The impacting particle's path through the target material is measured as the stopping range (R). The distance between the target's surface's starting point and 80 percent of the Bragg peak is another way to calculate the range values in proton treatment. The continuous slowing down approximation (CSDA) may be used to estimate the particle range in the target material [19]:

$$R(E) = \int_E^0 -\frac{1}{S(E)} dE \quad (5)$$

The stopping time is defined as the time required to stop the charged particle in a medium and it can be calculated from the following integral relationship [20]:

$$t(E) = \int_E^0 -\frac{1}{v S(E)} dE \quad (6)$$

where v is the ion velocity.

3. RESULTS AND DISCUSSION

The mean ionization potential was calculated for the constituent elements of water and studied human tissues using Gaussian 09W program for a number of basis sets which are 3-21G, 6-31G, 6-311G, LanL2DZ, LanL2MB, and SDD, mean ionization potential calculations are listed in Table 1 in eV units.

Table 1: Mean Ionization Potential Of Water, Lung, Bladder, And Intestine By Different Basis Sets

Tissue	Basis sets					
	3-21G	6-31G	6-311G	LanL2DZ	LanL2MB	SDD
Water	88.19	88.98	89.05	88.84	86.75	88.83
Lung	137.82	139.60	139.56	129.24	125.01	137.79
Bladder	138.34	140.06	140.01	129.34	125.14	137.32
Intestine	135.56	137.18	137.14	131.69	127.32	136.29

Figure 2, Section A, shows the relationship between the charge density distribution of orbital electrons in the atoms of the elements that make up water and the studied tissues in (e/a_0) unit, and the ratio of the radial distance to the Bohr radius a_0 , while Section B shows the relationship of the electron charge density distribution with the energy of the proton. The charge density distribution curves contain several peaks representing the centers of the electronic shell in each atom, and all curves start from zero where the nucleus of the atom is, and we also note that the hydrogen atom has the lowest value for the distribution of the electronic charge density because it contains only one electron, which makes its contribution to stopping The proton in the studied human tissues is very few, while the atoms of chlorine and potassium have the largest number of electrons among the constituent atoms, so they have the greatest values for the distribution of charge density, which makes their great contribution to stopping the proton.

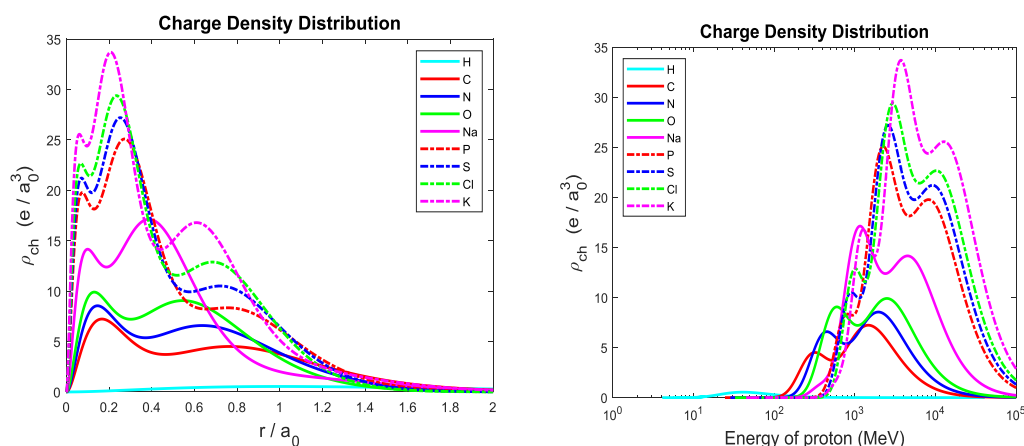


Figure 1 : Charge Density Distribution Of Elements In Water And Studied Human Body Tissues

The stopping power, range, and stopping time were calculated (in Table 3, and Figures 1, 2, and 3) using Bethe formula and density functional theory for water, lung, bladder,

and intestine with a proton energy range from 10^{-2} MeV to 10^3 MeV, Where the Bethe equation (Eq. 1) was used to calculate the stopping power of each of the elements that make up the water and lung, bladder, and intestine, then the stopping power for each of water and tissues was calculated from the Bragg equation (Eq. 4), and the weight ratios listed in Table 2.

Table 2: Weight Ratios Of Elements In Water And Studied Human Body Tissues

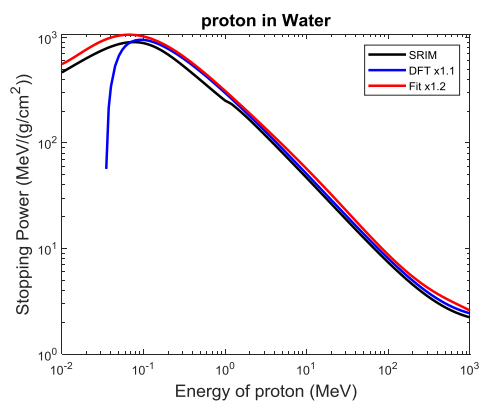
Tissue	H	C	N	O	Na	P	S	Cl	K
Water	0.112	-	-	0.888	-	-	-	-	-
Lung	0.007	0.089	0.031	0.846	0.003	0.004	0.007	0.008	0.006
Bladder	0.007	0.081	0.026	0.858	0.003	0.004	0.005	0.007	0.008
Intestine	0.008	0.099	0.022	0.858	0.002	0.002	0.002	0.005	0.003

The calculations of the stopping power of water, lung, bladder, and intestine are represented in Figure 1 in Section A, B, C and D respectively, the black curve represents the calculations of the global program SRIM-2013 and the blue curve represents the calculations of the relative Beth equation using the density functional theory, while the red curve represents the calculations of the curve fitting formula. All calculations for the blue and red curves have been multiplied by coefficients to show the difference between the curves because they are very similar. The calculations of the stopping power are directly proportional to the energy of the projectile (proton), as it increases with the increase of energy up to the maximum value of the stopping power. Else, then, the stopping power decreases with increasing proton energy. The correlation coefficient between the practical calculations of the SRIM-2013 program and the theoretical calculations are listed below each section of Figure 1. The values of the correlation coefficient show a good agreement between the calculations of the SRIM-2013 program and the calculations of the current study, especially in the high energies region (1 – 1000 MeV).

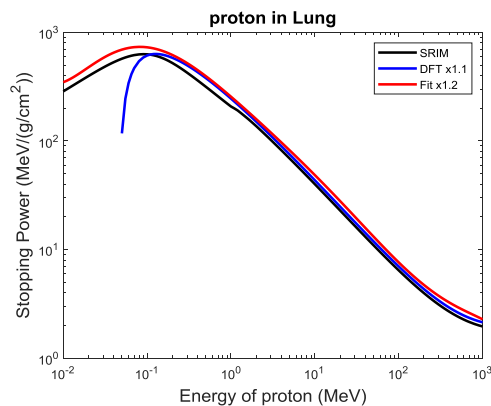
Table 3: Stopping Power Calculations S_{total} for Proton in Water And Studied Human Body Tissues

Proton energy(MeV)	S_{total} (MeV cm ² /g)			
	Water	Lung	Bladder	Intestine
0.01	-9844.7612	-11141.9148	-11162.6750	-11074.2823
0.02	-2148.9928	-3056.8217	-3067.0356	-3021.4691
0.05	606.9184	106.6873	102.6895	121.6411
0.07	818.1915	424.9167	422.0841	435.8114
0.1	858.1965	556.2108	554.2450	563.9954
0.2	706.5357	529.5924	528.6260	533.6390
0.5	429.4418	344.9190	344.5410	346.6196
0.7	345.3144	281.3256	281.0579	282.5620
1	270.3860	222.9037	222.7179	223.7854
2	163.1681	136.7943	136.7029	137.2512
5	80.2856	68.3110	68.2752	68.5028
7	61.3826	52.4420	52.4165	52.5815
10	46.0344	39.4787	39.4609	39.5784
20	26.1813	22.5899	22.5810	22.6421
50	12.4774	10.8319	10.8283	10.8546
70	9.5776	8.3298	8.3271	8.3467
100	7.3013	6.3611	6.3592	6.3736
200	4.4982	3.9303	3.9292	3.9376

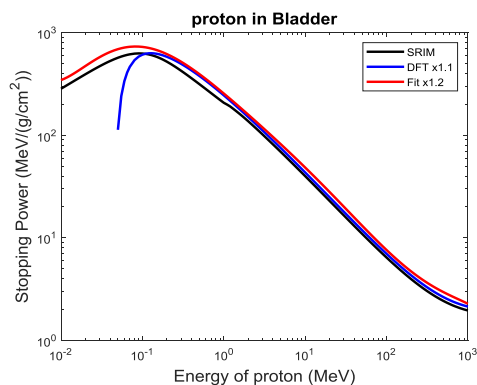
500	2.7463	2.4073	2.4068	2.4116
600	2.5582	2.2439	2.2433	2.2478
700	2.4285	2.1312	2.1307	2.1349
800	2.3353	2.0503	2.0499	2.0538
900	2.2664	1.9906	1.9902	1.9940
1000	2.2143	1.9456	1.9452	1.9489



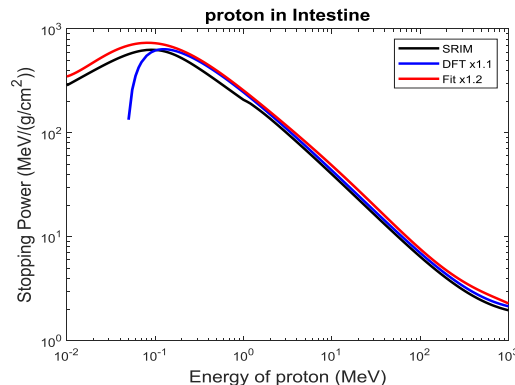
(A) $R_c = 0.9369$



(B) $R_c = 0.9464$



(C) $R_c = 0.9457$



(D) $R_c = 0.9504$

Figure 2: Rang calculations of electron in (A) water, (B) Lung, (C) Bladder, and (D) Intestine

The range and stopping time calculations calculated by equations (Eq. 5) and (Eq. 6) for water, lung, bladder and intestine are represented in Figure 2 and 3 in Section A, B, C and D respectively, and in the same order and colors as Figure 1 for stopping power, The range and stopping time is directly proportional to energy of proton, as it increases with the increase in energy. The correlation coefficient between the practical calculations of SRIM-2013 program and the theoretical calculations are listed at the bottom of each section of Figures 2 and 3, and they show the complete agreement between the calculations of the SRIM-2013 program and the calculations of the current study.

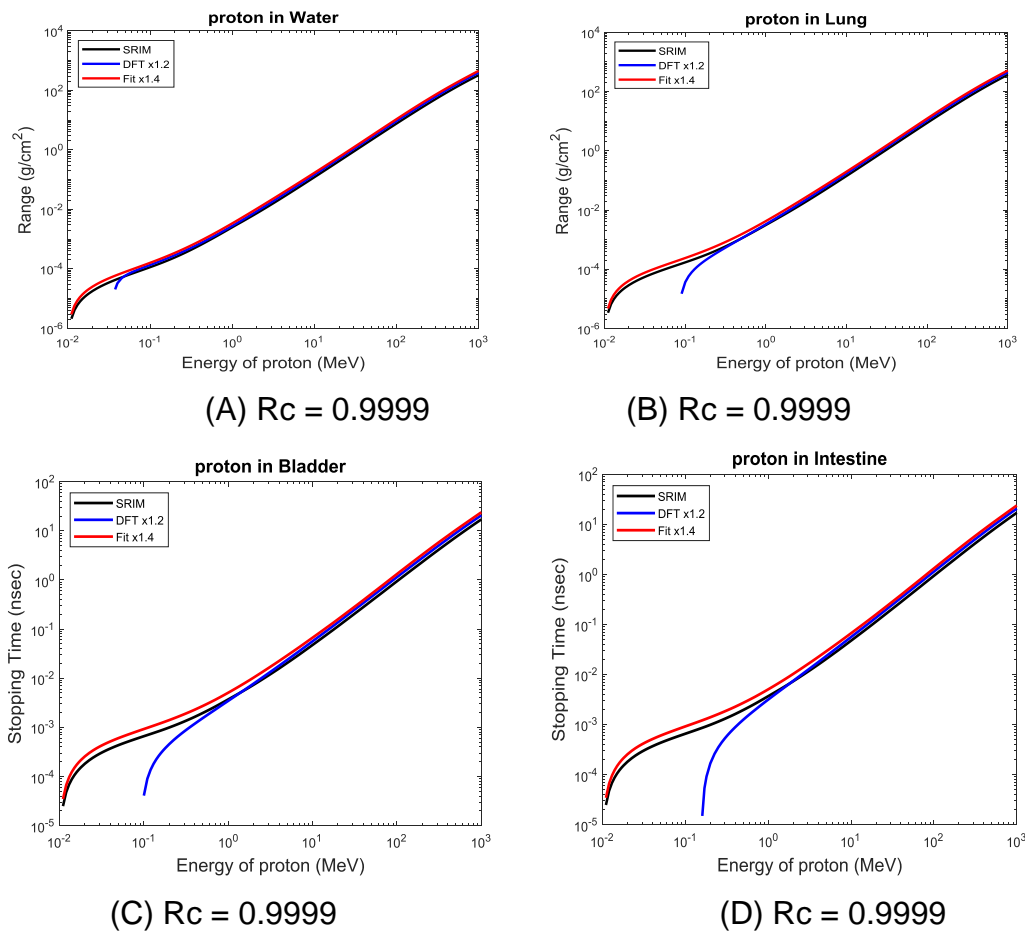


Figure 3: Stopping time calculations of electron in (A) water, (B) Lung, (C) Bladder, and (D) Intestine

4. CONCLUSIONS

The research results that we obtained to calculate the total stopping power by using Bethe equation by density functional theory and with an energy range (0.01-1000) MeV, it was discovered that the stopping power increases at low energies less than 0.1 MeV and decreases with an increase in energy greater than 0.1 MeV, where it was discovered through calculations that they depend on the projectile speed. It was found that the results of the curve match are near to the practical findings SRIM-2013 with about comparable correlation coefficients by applying the Bethe equation to compute the total stopping power in the study tissue. $R_c = 0.9$.

References

1. J. C. Ashley, (1991). Optical-data model for the stopping power of condensed matter for protons and antiprotons. *Journal of Physics: Condensed Matter*, 3(16), 2741–2753. H. Bethe (1930). *Zur Theorie des Durchgangs schneller Korpuskularstrahlen durch Materie.*, 397(3), 325–400.
2. W. H. Bragg; R. Kleeman, (1905). XXXIX. *On the α particles of radium, and their loss of range in passing through various atoms and molecules*. *Philosophical Magazine Series 6*, 10(57), 318–340.

3. C.F. Bunge; J.A. Barrientos; A.V. Bunge (1993). Roothaan-Hartree-Fock Ground-State Atomic Wave Functions: Slater-Type Orbital Expansions and Expectation Values for $Z = 2-54$, 53(1), 113–162.
4. R. Cabrera-Trujillo; S. A. Cruz; J. Oddershede; J. R. Sabin; (1997). Bethe theory of stopping incorporating electronic excitations of partially stripped projectiles. *Physical Review A*, 55(4), 2864–2872.
5. A. Dawidowska; M. P. Ferszt; A. Konefał; (2014). The determination of a dose deposited in reference medium due to (p,n) reaction occurring during proton therapy. *Reports of Practical Oncology & Radiotherapy*, 19(1), S3–S8.
6. D. Emfietzoglou; I. Kyriakou; I. Abril; R. Garcia-Molina; I.D. Petsalakis; H. Nikjoo; A. Pathak (2009). Electron inelastic mean free paths in biological matter based on dielectric theory and local-field corrections, 267(1), 45–52.
7. A. Ferrari, (2005). *Fluka: A Multi-particle Transport Code: (Program Version 2005)*. CERN.
8. P. L. Grande; G. Schiwietz (2009). Convolution approximation for the energy loss, ionization probability and straggling of fast ions. , 267(6), 859–865.
9. K. M. Hanson; J. N. Bradbury; T. M. Cannon, R. L. Hutson; D. B. Laubacher; R. J.Macek; M. A. Paciotti; C. A. Taylor, (1981). Computed tomography using proton energy loss. *Physics in Medicine and Biology*, 26(6), 965–983.
10. K. M. Hanson; J. N. Bradbury; R. A. Koeppe, R. J. Macek; D. R. Machen; R. Morgado, M. A. Paciotti; S. A. Sandford and V. W. Stewar (1982). Proton computed tomography of human specimens. *Physics in Medicine and Biology*, 27(1), 25–36.
11. N. Bohr (1948). On The Notions of Causality and Complementarity, 2(3-4), 312–319.
12. W. Brandt; (1975). *Atomic Collisions in Solids*, Plenum Press, New York, Vol. I, p. 261.
13. B. S. Yarlagadda; J. E. Robinson; W. Brandt; (1978). Effective-charge theory and the electronic stopping power of solids. *Physical Review B*, 17(9), 3473–3483.
14. F. Salvat; (2022). Bethe stopping-power formula and its corrections. *Physical Review A*, 106(3), 032809.
15. H. Sugiyama; (1981). Electronic stopping power formula for intermediate energies. *Radiation Effects*, 56(3-4), 205–211.
16. M. C. Tufan; A. Koroglu; H. Gumus; (2005). Stopping power calculations for partially stripped projectiles in high energy region. *Acta Phys. Pol. A* 107(3), 459–472.
17. D. I. Thwaites (1983). Bragg's Rule of Stopping Power Additivity: A Compilation and Summary of Results. *Radiation Research*, 95(3), 495–518.
18. S. M. Kheradmand; R. Machrafi; (2020). Development of a new code for stopping power and CSDA range calculation of incident charged particles, part A: Electron and positron. *Applied Radiation and Isotopes*, 161, 109145.
19. J. E. Turner; (2008). *Atoms, radiation, and radiation protection*. John Wiley & Sons.